Applicability Limits of Operational Modal Analysis to Operational Wind Turbines

D. Tcherniak[+], S. Chauhan[+], M.H. Hansen*

[+] Bruel & Kjaer Sound and Vibration Measurement A/S
Skodsborgvej 307, DK-2850, Naerum, Denmark

* Wind Energy Division, Risø DTU National Laboratory for Sustainable Energy,
Frederiksborgvej 399, DK-4000, Roskilde, Denmark

Email: dtcherniak@bksv.com, schauhan@bksv.com, mhha@risoe.dtu.dk

Nomenclature

f	Frequency
ω	Circular frequency
t	Time
$\{F(\omega)\}$	Vector of excitation force spectra (input)
$\{X(\omega)\}$	Vector of response spectra (output)
$[G_{FF}(\omega)]$, $[G_{XX}(\omega)]$	Cross-spectra matrices of forces and responses respectively
$S_u(f)$	Auto- or cross-spectra of incident wind fluctuations
$\overline{U}$	Mean wind speed
σ_u^2	Standard deviation of wind speed fluctuations
r_K	Radius of point K on a blade
$\kappa(\tau)$	Auto- or cross-correlation functions
$\gamma_{AB}^2(\omega)$	Coherence of aerodynamic forces (or wind speed fluctuations) at points A and B

Abstract

Operational Modal Analysis (OMA) is one of the branches of experimental modal analysis which allows extracting modal parameters based on measuring only the responses of a structure under ambient or operational excitation which is not needed to be measured. This makes OMA extremely attractive to modal analysis of big structures such as wind turbines where providing measured excitation force is an extremely difficult task.

One of the main OMA assumption concerning the excitation is that it is distributed randomly both temporally and spatially. Obviously, closer the real excitation is to the assumed one, better modal parameter estimation one can expect. Traditionally, wind excitation is considered as a perfect excitation obeying the OMA assumptions. However, the present study shows that the aeroelastic phenomena due to rotor rotation dramatically changes the character of aerodynamic excitation and sets limitations on the applicability of OMA to operational wind turbines.

The main purpose of the study is to warn the experimentalists about these limitations and discuss possible ways of dealing with them.

Introduction

The ability of Operational Modal Analysis to extract modal parameters of a structure under operation and without measuring excitation forces makes the technique extremely attractive to the application on wind turbines. First of all, a wind turbine is a huge structure where providing measured excitation is a challenging task. Secondly, since

OMA can be applied to a structure under operation, it promises to provide experimental values for *operational* natural frequencies and *operational* aerodynamic damping which differ from the ones at standstill and are otherwise difficult to obtain. At the same time a wind turbine is naturally subjected to aerodynamic forces due to wind turbulence, which have a broadband spectrum and properly excite wind turbine modes.

It's not incorrect to state that wind turbines have played a key role in developing OMA to a level where it currently stands. Though utilization of output only measurements for system identification goes back to 1970s, it wasn't till early 1990s that the science of OMA developed to an extent where it started getting applied to huge civil structures. This was result of research activities carried out in early 1990s at Wind Energy Research Organization, Sandia National Labs, USA; where by, while trying to understand the dynamics of wind turbines, James et al. proposed the NExT framework [1], that laid down the foundations of Operational Modal Analysis as it is understood now. As a part of this research, NExT was applied to vertical and horizontal axis wind turbines [1, 2], with varying degree of success. It was following this research that immense potential of output-only system identification techniques was realized, and subsequently applied to variety of civil structures including buildings, bridges, stadiums etc.

Having played such an important role in shaping OMA techniques, it's surprising to note that there wasn't much follow up to this pioneering work in understanding wind turbine dynamics by utilizing OMA techniques. It turns out that application of OMA to wind turbines is not a straight forward task due to a number of reasons, including presence of considerable aeroelastic effects, presence of rotational components in the excitation forces and time-varying nature of the wind turbine structure. These effects present considerable challenge for application of OMA techniques to wind turbines as they push the limits of these techniques by stretching the very basic assumptions that form the core of OMA.

A closer look onto OMA application to operational wind turbines reveals a number of inherent problems. First of all, the assumption of *structure time invariance* is violated. This assumption is distinctive to any kind of experimental modal analysis methods, and states that the object under test must not change during the test duration (or at least these changes should not be significant). In case of operational wind turbine this is not true: a wind turbine structure consists of substructures which move with respect to each other while the wind turbine operates: the nacelle rotates about the tower (which is characterized by the yaw angle); the rotor rotates about its axis; the blades' pitch may change depending on wind turbine type and operating conditions. Different methods can be applied to deal with time varying nature of the structure: For yaw and pitch, for example, periods of time when these angles do not change or change insignificantly can be selected for the analysis; a simple coordinate transformation can be performed in order to account for yaw angle; averaged characteristic value of pitch angle can be used while accepting that the obtained modal parameters are "smeared" due to blades pitching during the test duration. It is more difficult to deal with rotor rotation. Including rotor rotation into the equations of motion of entire wind turbine causes the mass, stiffness and gyroscopic matrices to be dependent on time. Formulating and solving the corresponding eigenvalue problem yields to time-dependent eigenvalues and eigenvectors, which do not have a meaning as modal frequencies, damping and mode shapes in traditional sense. Fortunately, by applying Coleman transformation [4-6], one can get rid of time dependencies in the equation of motion and obtain meaningful modal parameters. The combination of Coleman transformation and Operational Modal Analysis is demonstrated in [7].

Another inherent problem of application of OMA to operational wind turbines is the violation of OMA assumption concerning the operational excitation forces. OMA sets three quite specific requirements to the excitation: the forces should have broadband frequency spectra; they have to be distributed over entire structure, and they have to be uncorrelated. Seemingly, the excitation due to wind turbulence is ideal for OMA. Indeed, the forces due to wind turbulence have almost uniform broadband spectra; they are uncorrelated and obviously excite entire structure. However, the effect of rotor rotation dramatically changes the nature of aerodynamic forces. First of all, the shape of the spectra transforms from being flat to a curve with prominent peaks at rotation frequency and its harmonics; the peaks' shape is not sharp but characterized by thick tails [8, 9]. Secondly, the forces appear to be quite correlated around the rotation frequency and its harmonics. The abovementioned reasons make the aerodynamic excitation much less suitable for OMA. The presented paper addresses this phenomenon.

The paper is built as follows: Section 1 briefly reminds the reader the main ideas and assumptions OMA is based on. Section 2 uses the analytical model of wind excitation based on von Karman spectrum, and derives the spectra of wind excitation forces and coherence between them; Section 3 demonstrates the same using the results of numerical simulation of wind/blades interaction of wind turbine under operation. In Section 4, the results are discussed and some conclusions are drawn.

1. Operational Modal Analysis: theory and main assumptions

OMA is a system identification technique based only on measured output responses. It does not require input force information but makes certain assumptions about the nature of the input excitation forces. Like any other technique, adherence to basic assumptions is the key to successful application of OMA techniques. Importance of these assumptions can be gauged by the fact that modal parameters obtained using OMA are obviously affected depending on how closely the actual conditions resemble the one supported by these basic assumptions. These assumptions are listed below:

1. Power spectra of the input forces are assumed to be broadband and smooth;
2. The input forces are assumed to be uncorrelated;
3. The forces are distributed over entire structure

In other words, *the excitation is assumed to be randomly distributed both temporally and spatially*.

Expression (1) gives the mathematical relationship between the vector of measured responses, $\{X(\omega)\}$ and vector of input forces, $\{F(\omega)\}$ in terms of the frequency response function (FRF) matrix $[H(\omega)]$ [3]:

$$\{X(\omega)\} = [H(\omega)]\{F(\omega)\}; \tag{1}$$

$$\{X(\omega)\}^H = \{F(\omega)\}^H [H(\omega)]^H . \tag{2}$$

Now multiplying (1) and (2)

$$\{X(\omega)\}\{X(\omega)\}^H = [H(\omega)]\{F(\omega)\}\{F(\omega)\}^H [H(\omega)]^H , \tag{3}$$

or with averaging,

$$[G_{XX}(\omega)] = [H(\omega)][G_{FF}(\omega)][H(\omega)]^H , \tag{4}$$

where $[G_{XX}(\omega)]$ is the matrix of output power spectra and $[G_{FF}(\omega)]$ is the input force power spectra matrix.

From the first two assumptions, it follows that

$$[G_{FF}(\omega)] \propto [I], \tag{5}$$

therefore the output power spectra $[G_{XX}(\omega)]$ is proportional to the product $[H(\omega)][H(\omega)]^H$ and the order of output power spectrum is twice that of the frequency response functions. Thus $[G_{XX}(\omega)]$ can be expressed in terms of frequency response functions as

$$[G_{XX}(\omega)] \propto [H(\omega)][I][H(\omega)]^H . \tag{6}$$

Partial fraction form of G_{XX} for particular locations p and q is given as

$$G_{pq}(\omega) = \sum_{k=1}^{N} \frac{R_{pqk}}{j\omega - \lambda_k} + \frac{R^*_{pqk}}{j\omega - \lambda^*_k} + \frac{S_{pqk}}{j\omega - (-\lambda_k)} + \frac{S^*_{pqk}}{j\omega - (-\lambda^*_k)} , \tag{7}$$

where R_{pqk} and S_{pqk} are k^{th} mathematical residue terms and are not to be confused with residue terms obtained using FRF based model as these term do not contain modal scaling information (since input force is not measured). It is important to note that this expression shows that power spectra *contains all information needed to define the modal model* of the system (except for modal scaling factor), *provided the loading assumptions are true*.

2. Frequency analysis of aerodynamic forces

In wind turbine engineering [8], it is typical to separate the loading due to the steady wind and loading due to wind speed fluctuation (i.e. turbulence). The first one is often called *deterministic* load component while the second is *stochastic*. The first component is characterized by the mean wind speed, which is considered to be time-constant

in the time scale over about 10 minutes. In this study, we consider it not possessing any broadband frequency content. The second component *has* broadband frequency content, and therefore has a key importance for Operational Modal Analysis due to its ability to provoke modal behavior of the wind turbine structure. The presented paper concerns only the stochastic loading.

The source of the stochastic loading is turbulence, a fluctuation in wind speed on a relatively fast time-scale typically less than about 10 minutes [8]. In other words, we assume the fluctuations of wind speed have a zero mean when averaging over 10 minutes. There are two main sources of turbulence: flow disturbance due to topographic features and thermal effects causing air masses to move vertically. These are obviously complex processes; therefore the description of turbulence is typically developed using its statistical properties.

Turbulence frequency spectrum is an important property of turbulence. There are several turbulence models used in wind turbine engineering; in this study we will refer to two of them; the first one is described by Kaimal spectrum (used in Section 3), the second one – by von Karman spectrum. In this section we use the formulation suggested by von Karman [10]:

$$\frac{f S_u(f)}{\sigma_u^2} = \frac{4L_u^x}{\overline{U}\left(1+70.8\left(\frac{f L_u^x}{\overline{U}}\right)^2\right)^{5/6}}, \tag{8}$$

where f is frequency, $S_u(f)$ is the autospectral density of the turbulence (its longitudinal component which is denoted by symbol u), σ_u is the standard deviation of wind speed variations about mean wind speed in longitudinal direction $\overline{U}$. Standard deviation σ_u and mean speed $\overline{U}$ are linked via *turbulence intensity* $I_u = \sigma_u / \overline{U}$. L_u^x is a turbulence *length scale*. Different national standards provide empiric expressions defining the values for the turbulence intensity and length scale; these values mainly depend on the elevation above the ground and the surface roughness. The blue line on Figure 1 shows a typical spectrum calculated according to (1) with L_u^x = 64.4 m (corresponding to the elevation greater then 30 m above the ground) and $\overline{U}$ = 8 m/s^2.

As it can be seen from the plot, most of the energy is distributed on the very lower frequencies, much below typical rotation frequencies (here set equal to 0.202Hz and denoted by "1p" on the frequency axis). On the higher frequencies the turbulent energy tend to dissipate as a heat, and the spectral density asymptotically approaches the limit $f^{-5/3}$ Hz.

As it was mentioned in Section 1, Operational Modal Analysis sets a number of requirements on structure excitation. In the case of wind turbine, the main excitation is due to wind-structure interaction; therefore it is important to understand the relation between the turbulence and the resulting aerodynamic forces. As it is stated in [8], it is usual to assume a *linear relation* between the *fluctuation* of the wind speed u incident on the aerofoil and the resulting loading *fluctuations* $\Delta L \propto u$. This assumption is correct for low wind speeds and becomes inaccurate for pitch regulated turbines as wind speed approaches cut-out value and breaks down for stall-regulated machines when wind speed can cause stall. In this section we will assume low wind speeds and therefore the linear relation between the wind speed fluctuation and the resulting loading, so the results will be given for wind speed fluctuation u, implying the forces behave similarly.

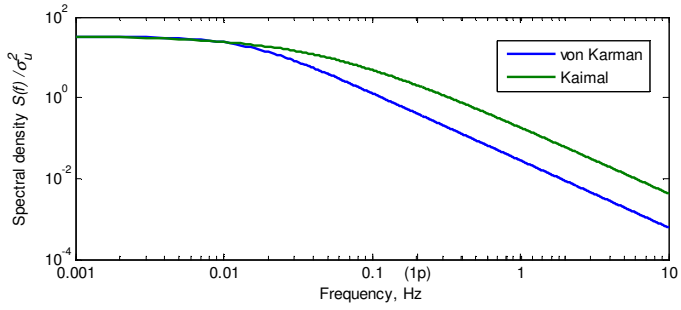

Figure 1: Normalized spectra: according to von Karman (blue) and Kaimal (green)

Following [8] and assuming that the fluid is incompressible, the turbulence is homogeneous and isotropic and using Taylor's hypothesis of "frozen turbulence", it is possible to obtain an analytical expressions for cross-correlation function of wind speed computed for points A and B on the blades (Figure 2).

In brief, the derivation is based on the use of Wiener-Khinchin theorem on power spectrum (8) which yields to analytical expression for the autocorrelation function at any fixed point in space; and then computing the cross-correlation function between points A_t and $B_{t+\tau}$ (Figure 2). Using the hypothesis of "frozen turbulence", instantaneous

wind fluctuation at $B_{t+\tau}$ is assumed to be equal to the wind fluctuation at point B_t'. The derived expression for correlation along vector s at $t = 0$ approximates the cross-correlation function between points A_t and $B_{t+\tau}$: $\kappa_u(\vec{s},0) = \kappa_u^o(r_1, r_2, \tau)$.

$$\kappa_u^o(r_1, r_2, \tau) = \\ = \frac{2\sigma_u^2}{\Gamma\left(\frac{1}{3}\right)}\left(\frac{s/2}{1.34L_u^x}\right)^{1/3}\left(K_{1/3}\left(\frac{s}{1.34L_u^x}\right) - \frac{s/2}{1.34L_u^x}\left(\frac{r_1^2 + r_2^2 - 2r_1 r_2\cos(\Omega\tau + k\cdot 2\pi/3)}{s^2}\right)K_{2/3}\left(\frac{s}{1.34L_u^x}\right)\right) \quad (9)$$

where interpretations for s, r_1, r_2 can be found on Figure 2a,b; K_v is Bessel function of second kind; and $k = 0$ if points A and B are on the same blade, k = -1 if blade with point A is moving before the blade with B and k = 1 for the opposite situation. As it can be seen from the triangle on Figure 2c,

$$s^2 = (\overline{U}\tau)^2 + r_1^2 + r_2^2 - 2r_1 r_2\cos(\Omega\tau + k\cdot 2\pi/3)\,. \quad (10)$$

Figure 3a shows autocorrelation function computed for the fixed point on the blade (i.e. points A and B coincide, $r_1 = r_2$ and $k = 0$) for different radii. The peaks at multiples of the period of rotor revolution T are due to high correlation of the incident wind speed with itself when a blade passes the same region of the rotor swept area.

Spectra of aerodynamic forces

Application of the Wiener-Khinchin theorem to expression (9) yields the power spectrum density (PSD) of the incident wind speed fluctuations; there is no implicit expression for the resulting integral, instead it can be approximated and estimated numerically. The PSDs of the corresponding autocorrelation functions are shown on Figure 3b.

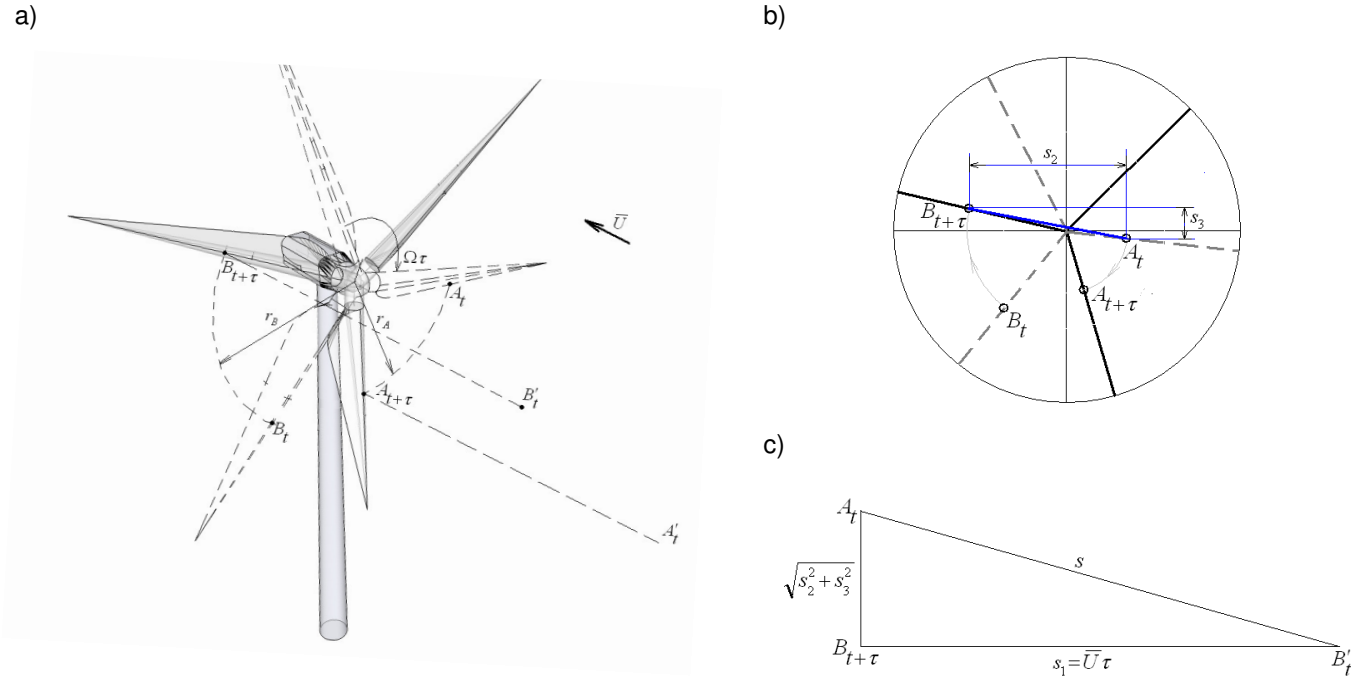

Figure 2. Points A and B are located at radii r_1 and r_2 respectively. A_t, B_t are the positions of the corresponding points at time t. a) Geometry of the wind turbine; b) View along the wind speed; c) Position triangle used for cross-spectrum calculation.

a)

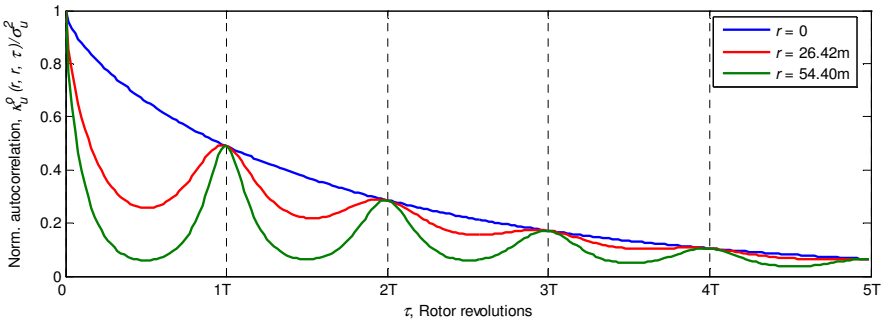

b)

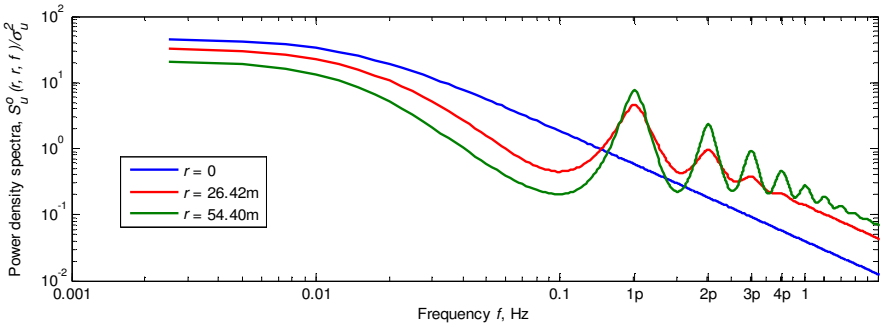

Figure 3. a) Normalized autocorrelation functions computed for the *fixed* point on the blade ($r_2 = r_1$ and $k = 0$), on the different radii (0, 26.42 and 54.40 m); b) Normalized PSD calculated for the autocorrelation functions shown above.

The following observations can be made:

1. The spectra have peaks at the fundamental frequency and its harmonics;
2. The peaks become more pronounced with increasing of radius r (with no peaks at $r = 0$);
3. The peaks are not sharp but have rather thick tails.

The physics of these phenomena can be explained by imagining a blade passing regions with higher or lower wind speed that generates periodicity of the incident wind speed and hence of the aerodynamic loading; increasing the ratio between the tangential speed of the point on a blade and the mean wind speed $\Omega r / \overline{U}$ will generate higher peaks and deeper troughs between the peaks. The center of the rotor experiences only mean wind therefore the spectrum there coincides with the spectrum of the turbulence (Figure 1, the blue curve).

The third listed feature of the PSD is the peak's thick tails. It is difficult to get a feeling about the nature of this phenomenon. The following explanation can be suggested: one can roughly approximate the autocorrelation function at $r \neq 0$ (Figure 3a) by a product of a decaying function like the blue curve (the autocorrelation at $r = 0$) and some periodic function. The latter consists of the infinite number of terms (due to the Bessel functions in (9)) which are periodic (due to periodicity of s, (10)) and have different periods (due to the different powers of the cosine function). In frequency domain, a product of two autocorrelation functions becomes a convolution of their spectra [11]. One has to imagine the spectrum of the first function (the blue curve on Figure 3b) convolved with the spectrum of the second one, which will have infinite number of sharp peaks at different frequencies. The result of the convolution will be "smearing" of the peaks into the smooth spectra shaped as "thick tails".

As it was mentioned above, the fluctuations of the aerodynamic loading is linearly proportional to the turbulence, meaning that the PSD of the aerodynamic forces will have the same shape as curves shown on Figure 3b. Thus, we can see that the excitation spectra are not flat in the frequency range of interest, and this therefore violates the first OMA assumption.

Correlation between aerodynamic forces

The second important OMA assumption is that the forces acting at different points of a structure must be uncorrelated (see Section 1). In this subsection we will estimate the correlation of the excitation forces by calculating the coherence between the wind speed fluctuations at different points on the same and different blades.

Coherence γ_{AB}^2 between incident wind speed fluctuation at points A and B on the rotating blades is

$$\gamma_{AB}^2(f) = \frac{\left|S_u^{AB}(f)\right|^2}{S_u^{AA}(f) S_u^{BB}(f)}, \tag{11}$$

where S_u^{AA} and S_u^{BB} are autospectra of wind turbulence at points A and B respectively and S_u^{AB} is cross-spectra between these points. The auto- and cross-spectra can be calculated from auto- and cross-correlation functions (9) applying Wiener-Khinchin theorem. Figure 4 shows the auto- and cross-correlation functions calculated at different points on different blades, corresponding auto- and cross-spectra, and the coherence.

The correlation functions are presented on Figure 4a. Cross-correlation functions computed for the points on different blades pass ahead the autocorrelation function: indeed, if for example, blade #1 experiences a gust at some segment of the rotor swept area, it will take it a full revolution (and time T) to experience the same gust again. However, for blade #2 which follows blade #1, it will take only $T/3$ to experience the same gust, and for blade #3 it will happen after $2T/3$. This explains the corresponding time lags of the black and magenta curves on Figure 4a.

The auto- and cross-spectra are obtained numerically for the corresponding auto- and cross-correlation functions; their magnitudes are shown on Figure 4b[1]. The cross-spectra for the cases when blade A follows blade B and B follows A are the same.

Coherence functions between the wind turbulence at points A and B if the points are located on different blades, are presented on Figure 4c. Similar to the spectra, the coherences have peaks at rotation frequency and its harmonics; the peaks are more pronounced for low harmonics and gradually decay at higher frequencies. Further, the peaks are not sharp but have rather thick tails; this makes the troughs between them quite narrow.

Thus, here one can claim the violation of the second OMA assumptions concerning the correlation between the excitation forces. As one can see, the assumption is strongly violated in the frequency range between 0.5p - 4.5p, leaving only narrow deeps between the peaks where the assumption is valid.

3. Analysis of the synthesized time data

As it was mentioned in Section 2, the presented analytical approach is only suitable for weak wind where the linear relation between aerodynamic force fluctuations and wind turbulence is valid. For higher wind speeds the analysis is usually performed in time domain by numerical simulation of wind-blade interaction.

Similar to [12], the simulations were performed using the nonlinear aeroelastic multi-body code HAWC2 [13]. A turbulence box with resolution 32 x 32 x 16384 was generated based on Kaimal turbulence spectrum with mean wind speed 18 m/s and turbulence intensity 5%. Figure 1 (green line) shows the corresponding spectrum calculated for this speed and L_{1u} = 150 m. The turbulence box corresponded to 12000 s of simulation. Aerodynamic forces at radii 26.42, 39.95 and 54.40 m in X- and Y- directions were calculated as functions of time; the analysis was done on the generated time histories, for X (along the wind) direction only.

[1] Note that the numerical approach suggested in [8] is suitable here since it assumes the symmetry of the correlation functions about $t = 0$. This is correct for auto-correlation functions and cross-correlations between the points on the same blade. The cross-correlation functions between the points on different blades (i.e. for $k \neq 0$) are not symmetric, see Figure 4a.

a)

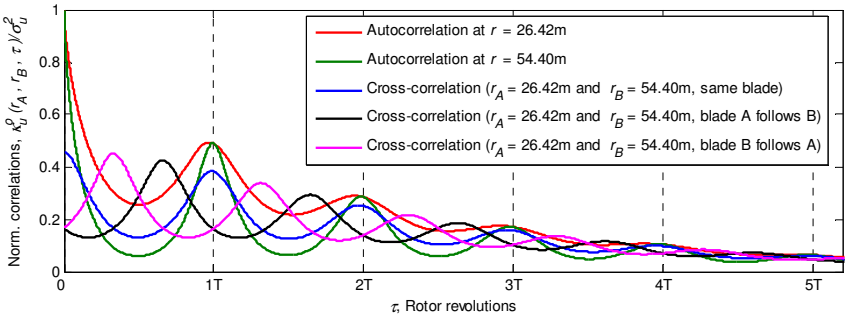

b)

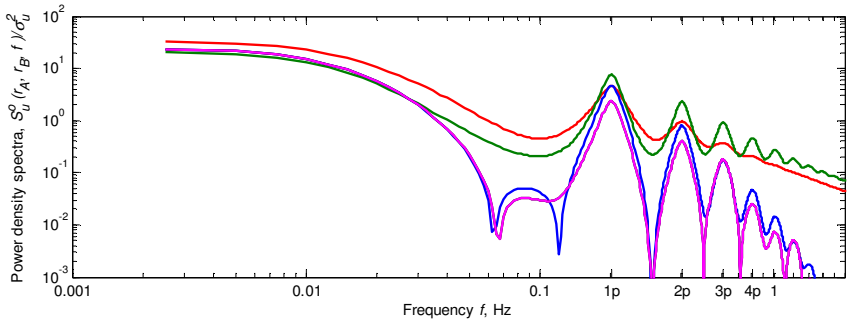

c)

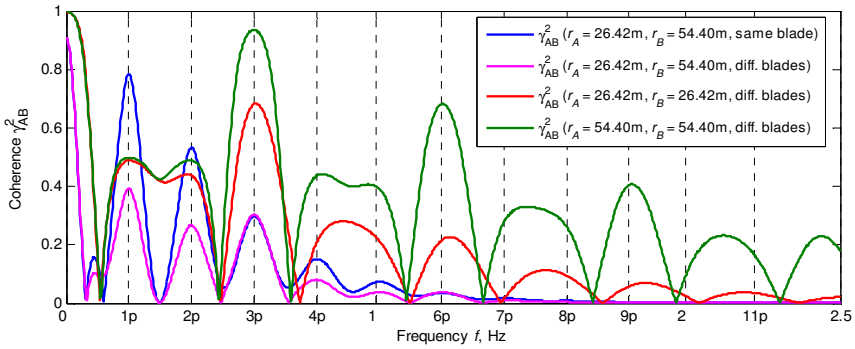

Figure 4. a) Auto- and cross-correlation functions; b) auto- and cross-spectra; c) coherence.

Figure 5 shows the autospectra of the aerodynamic forces acting in X-direction, and Figure 6 shows the coherence between aerodynamic forces simulated at different points on the blades.

Obviously, the results obtained analytically and numerically are not directly comparable. First of all, for analytical case the spectra and coherence of *wind fluctuations* are shown where for the numerical case the resulting *aerodynamic forces* are presented. Secondly, the wind speed is different (modest 8 m/s for analytical case vs. strong 18 m/s wind for the numerical case). Thirdly, two different wind turbulence spectra are used: von Karman for the analytical case and Kaimal for the numerical simulations. Despite this, qualitatively, the shape of the spectra and coherence functions look very similar. In both case they are characterized by peaks at rotation frequency and its harmonics, with their heights decreasing with frequency increase. At low frequencies (1p-4p) the peaks clearly exhibit the “thick tails”.

The shape of the coherence functions computed for the two cases is more different: in the numerical case the sharp peaks present even on high harmonics. Otherwise, there are similarities, too. For example, the coherence between the points on the same radius on the different blades (Figure 6c,d) is generally higher compare to the one between the points at different radii (Figure 6a,b).

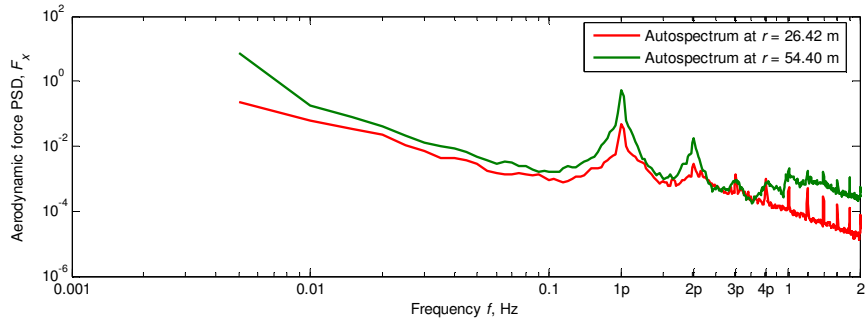

Figure 5. Power spectral density of the simulated aerodynamic forces in X direction.

4. Discussion and Conclusion

In the study it is demonstrated both analytically and numerically, for weak and strong wind excitation that for *operational* wind turbine:

1) The spectra of aerodynamic forces are not flat but are characterized by peaks at rotational frequency and few lower harmonics. The peaks are not sharp but have thick tails.
2) The forces acting at different points on the blades are highly correlated on the rotational frequency and its lower harmonics.

This means that two important OMA assumptions are not satisfied in a number of frequency regions around the rotational frequency and its lower harmonics. Thus one must not expect OMA to provide correct results in these frequency regions. Some important modes of modern wind turbines (e.g. drivetrain mode, first tower modes, first flapwise modes) are located in these regions for the nominal rotational speeds [14], so one has to be careful trying to identify them using OMA.

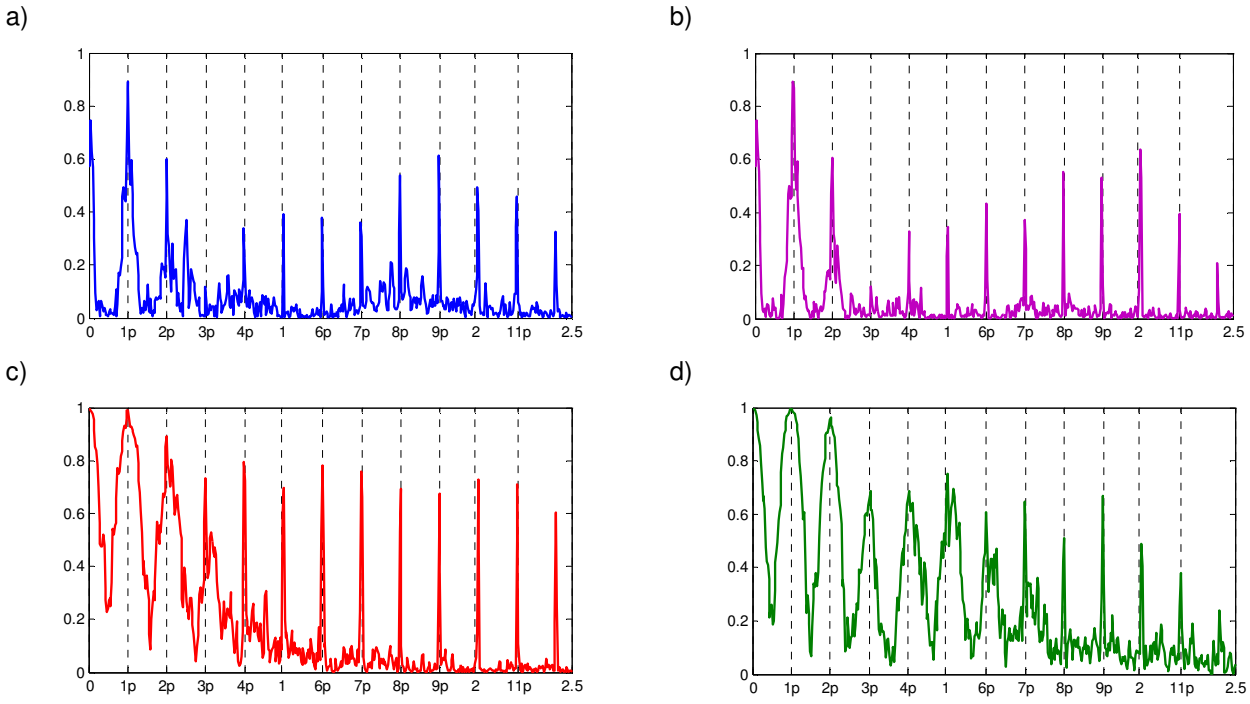

Figure 6. Coherence of the simulated aerodynamic forces. Same colour scheme as on Figure 4c.

It is important to note that application of *tone removing* methods (e.g. based on synchronous averaging, [15]) cannot be considered as a proper solution, as these methods work well only for sharp peaks but will not help in this case due to the "thick tails" phenomenon.

From a first glance, a use of run-up and run-down events looks attractive but, first of all, these events are rather short compare to the acquisition time required for data collection for proper OMA (about 10 minutes if the lowest frequency of interest is 0.2-0.4 Hz). Secondly, a wind turbine engineer is typically interested in the dependency of modal parameter on the rotor speed; in the case of run-up/run-down events, only averaged modal characteristics can be obtained.

In order to solve the problem, one can consider a careful planning of the experiment, constructing the test matrix in a way to avoid the modal frequencies (which are typically known from FEA) to be in the vicinity of rotor speed and its lowest harmonics. This means that only few modes can be estimated with higher degree of confidentiality for a given rotor speed, while another rotor speed will be suitable for another set of modes.

Amongst recently suggested methods, operational modal analysis based on transmissibility functions [16] appears very appealing. One of the main advantages of this method is its insensitivity to colored excitation spectra. However, so far this method is still under development and is not ready for industrial applications.

Literature

[1] G.H. James, T.G. Carne, J.P. Lauffer (1995), *The Natural Excitation Technique (NExT) for Modal Parameter Extraction from Operating Structures*, *Modal analysis: The International Journal of Analytical and Experimental Modal Analysis 10, 260-277*.

[2] G.H. James (1994), *Extraction of Modal Parameters from an Operating HAWT using the Natural Excitation Technique (NExT)*, *Proceedings of the 13th ASME Wind Energy Symposium, New Orleans, LA*.

[3] J. Bendat, A. Piersol (1986), *Random Data: Analysis and Measurement Procedures*, 2nd edition, Wiley, New York.

[4] M.H. Hansen (2003), *Improved Modal Dynamics of Wind Turbines to Avoid Stall-induced Vibrations*, *Wind Energ.* 2003; **6**: 179-195

[5] M.H. Hansen (2006), *Two Methods for Estimating Aeroelastic Damping of Operational Wind Turbine Modes from Experiment*, *Wind Energ.* 2006; **9**: 179-191

[6] G. Bir (2008), *Multiblade Coordinate Transformation and its Application to Wind Turbine Analysis*, *Proceedings of 2008 ASME Wind Energy Symposium, Reno, Nevada, USA, Jan. 7-10, 2008*

[7] D. Tcherniak, S. Chauhan, M. Rosseti, I. Font, J. Basurko, O. Salgado (2010), *Output-only Modal Analysis on Operating Wind Turbines: Application to Simulated Data*, Submitted to *European Wind Energy Congress, Warsaw Apr. 2010*

[8] T.Burton, D. Sharpe, N. Jenkins, E.Bossanyi (2001), *Wind Energy Handbook*, John Wiley & Sons, West Sussex, England

[9] L. Kristensen, S. Frandsen (1982), *Model for Power Spectra of the Blade of a Wind Turbine Measured from the Moving Frame of Reference*, *Journal of Wind Engineering and Industrial Aerodynamics, 10 (1982) 249-262*

[10] T. von Karman (1948), *Progress in the statistical theory of turbulence, Proc. Natl. Acad. Sci. (U.S.), 34 (1948) 530-539*

[11] R.B. Randall (1987), *Frequency Analysis*, 3rd edition, Bruel and Kjaer

[12] S. Chauhan, M. H. Hansen, D. Tcherniak (2009), *Application of Operational Modal Analysis and Blind Source Separation /Independent Component Analysis Techniques to Wind Turbines, Proceedings of XXVII International Modal Analysis Conference, Orlando (FL), USA, Feb. 2009*

[13] T.J. Larsen, H.A. Madsen, A.M. Hansen, K. Thomsen (2005), *Investigations of stability effects of an offshore wind turbine using the new aeroelastic code HAWC2*, *Proceedings of Copenhagen Offshore Wind 2005*, *Copenhagen*, *Denmark*, *p.p.25–28*.

[14] M.H. Hansen (2007), *Aeroelastic Instability Problems for Wind Turbines*, *Wind Energ.* 2007; **10**: 551-577

[15] B. Peeters, B. Cornelis, K. Janssens, H. Van der Auweraer (2007), *Removing disturbing harmonics in operational modal analysis*, *Proceedings of International Operational Modal Analysis Conference, Copenhagen, Denmark, 2007*

[16] C. Devriendt, T. De Troyer, G. De Sitter, P. Guillaume (2008), *Automated operational modal analysis using transmissibility functions*, *Proceedings of International Seminar on Modal Analysis, Leuven, Belgium Sep. 2008*